

Electronic Supplementary Information

Self-Assembled Conjugated Polyelectrolyte-Surfactant Complexes as Efficient Cathode Interlayer Materials for Bulk Heterojunction Organic Solar Cells

Michèle Chevrier,^{ab} Judith E. Houston,^c Jurgen Kesters,^d Niko Van den Brande,^e Ann E. Terry,^f Sébastien Richeter,^a Ahmad Mehdi,^a Olivier Coulembier,^b Philippe Dubois,^b Roberto Lazzaroni,^g Bruno Van Mele,^e Wouter Maes,^{*d} Rachel C. Evans^{*ch} and Sébastien Clément^{*a}

^a Institut Charles Gerhardt – UMR 5253, Equipe Chimie Moléculaire et Organisation du Solide, Université Montpellier 2 – CC1701, Place Eugène Bataillon, F-34095 Montpellier Cedex 05, France. E-mail: sebastien.clement1@umontpellier.fr; Tel: +33467143971.

^b Laboratory for Polymeric and Composites Materials, Center for Innovation in Materials and Polymers, Research Institute for Science and Engineering of Materials, University of Mons – UMONS, 23 Place du Parc, B-7000 Mons, Belgium.

^c School of Chemistry, The University of Dublin, Trinity College, Dublin 2, Ireland. E-mail: raevans@tcd.ie

^d Institute for Materials Research (IMO), Design & Synthesis of Organic Semiconductors (DSOS), Hasselt University, Agoralaan 1–Building D, B-3590 Diepenbeek, Belgium. E-mail: wouter.maes@uhasselt.be

^e Physical Chemistry and Polymer Science (FYSC), Vrije Universiteit Brussel (VUB), Pleinlaan 2, B-1050 Brussels, Belgium.

^f ISIS-CCLRC, Rutherford Appleton Laboratory, Chilton, Oxon OX11 0QX, United Kingdom.

^g Laboratory for Chemistry of Novel Materials, Center for Innovation in Materials and Polymers, Research Institute for Science and Engineering of Materials, University of Mons – UMONS, 23 Place du Parc, B-7000 Mons, Belgium.

^h Centre for Research on Adaptive Nanostructures and Nanodevices (CRANN), Trinity College Dublin, Dublin 2, Ireland.

Table of contents

Photoactive layer components	P.3
^1H NMR spectrum of P3HTPMe₃,DS in CD ₃ OD	P.4
$^{13}\text{C}\{^1\text{H}\}$ NMR spectrum of P3HTPMe₃,DS in CD ₃ OD	P.4
$^{31}\text{P}\{^1\text{H}\}$ NMR spectrum of P3HTPMe₃,DS in CD ₃ OD	P.5
^1H NMR spectrum of P3HT-<i>b</i>-P3HTPMe₃,DS in CDCl ₃	P.5
^1H NMR spectrum of P3HT-<i>b</i>-P3HTPMe₃,DS in DMSO- <i>d</i> ₆	P.6
$^{13}\text{C}\{^1\text{H}\}$ NMR spectrum of P3HT-<i>b</i>-P3HTPMe₃,DS in CDCl ₃	P.6
$^{31}\text{P}\{^1\text{H}\}$ NMR spectrum of P3HT-<i>b</i>-P3HTPMe₃,DS in CDCl ₃	P.7
SANS data analysis	P.8
SANS data analysis: Rigid Cylinder model details	P.8
SANS data analysis: Flexible Cylinder model details	P.9
SANS data analysis: Lamellar Sheet model details	P.11
SANS data analysis: Core Shell Cylinder model details	P.11
SANS data analysis: Aggregation numbers	P.13
SANS data analysis: Holtzer plot of SANS data for P3HTPMe₃ in <i>d</i> ₄ -MeOD	P.13
SANS data analysis: Rigid Cylinder model fitting of P3HTPMe₃ in <i>d</i> ₄ -MeOD	P.13
SANS data analysis: Summary of fitting parameters	P.14

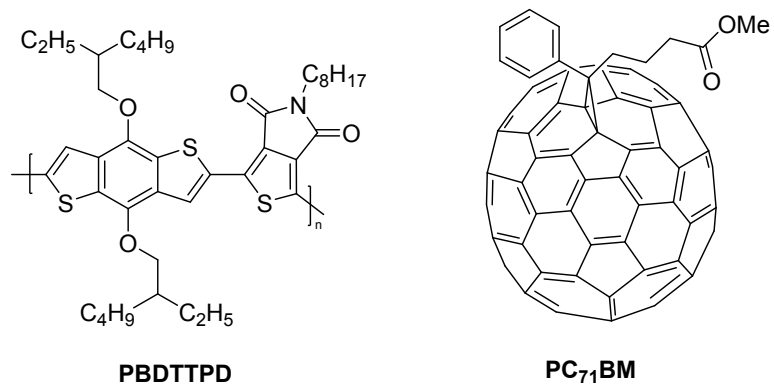


Fig. S1. Photoactive layer components.

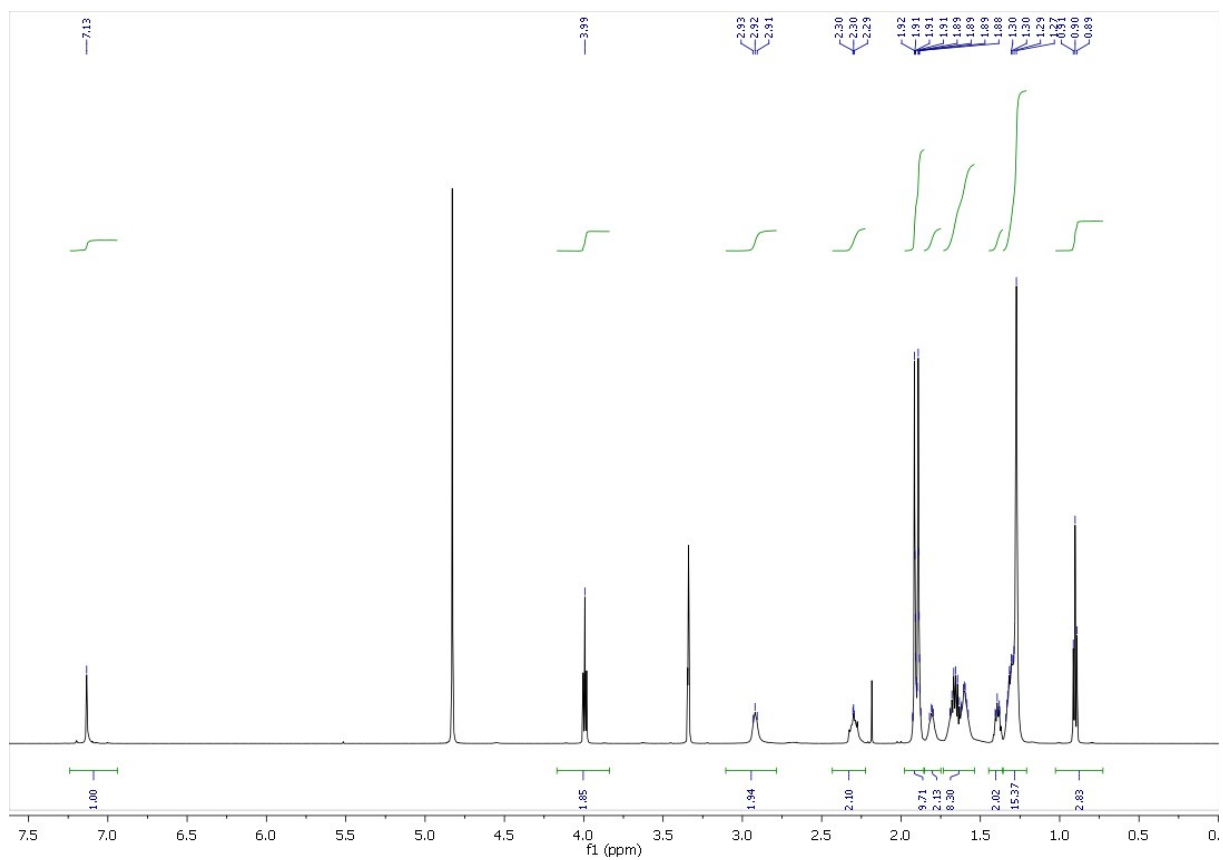


Fig. S2. ^1H NMR spectrum of **P3HTPMe₃,DS** in CD_3OD .

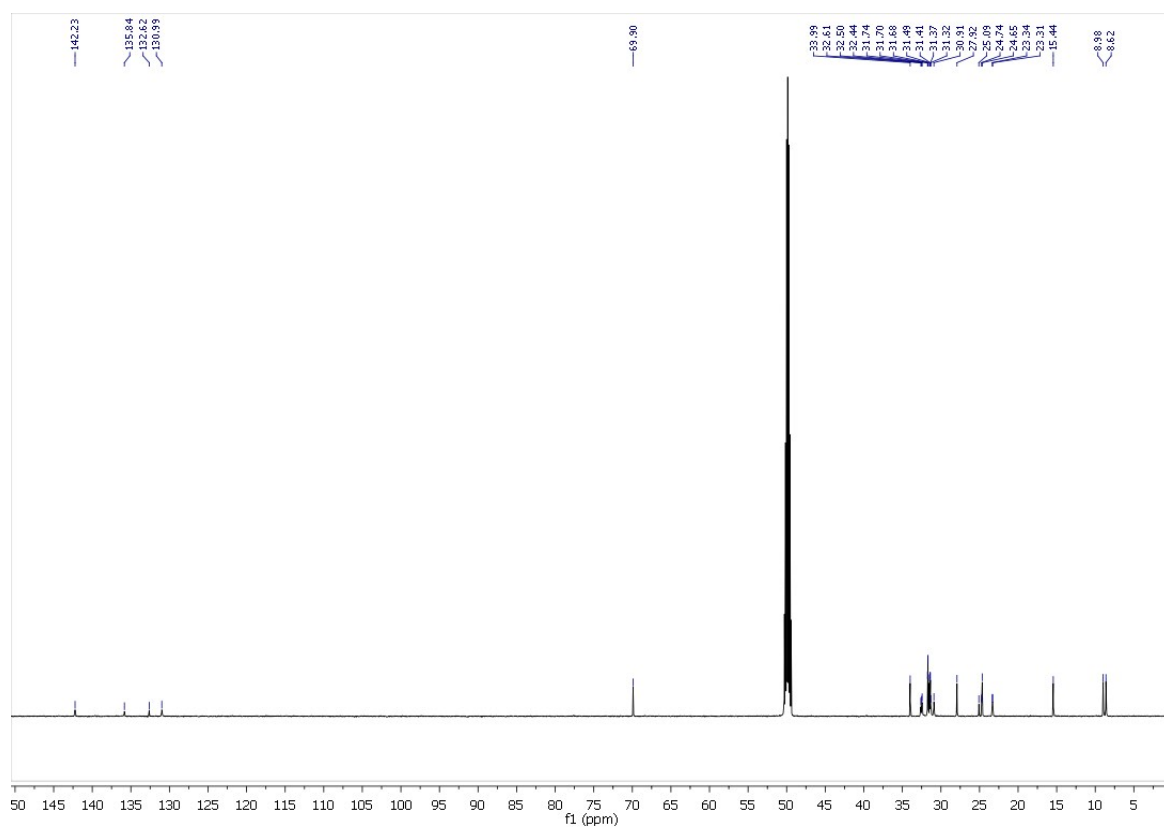


Fig. S3. $^{13}\text{C}\{^1\text{H}\}$ NMR spectrum of **P3HTPMe₃,DS** in CD_3OD .

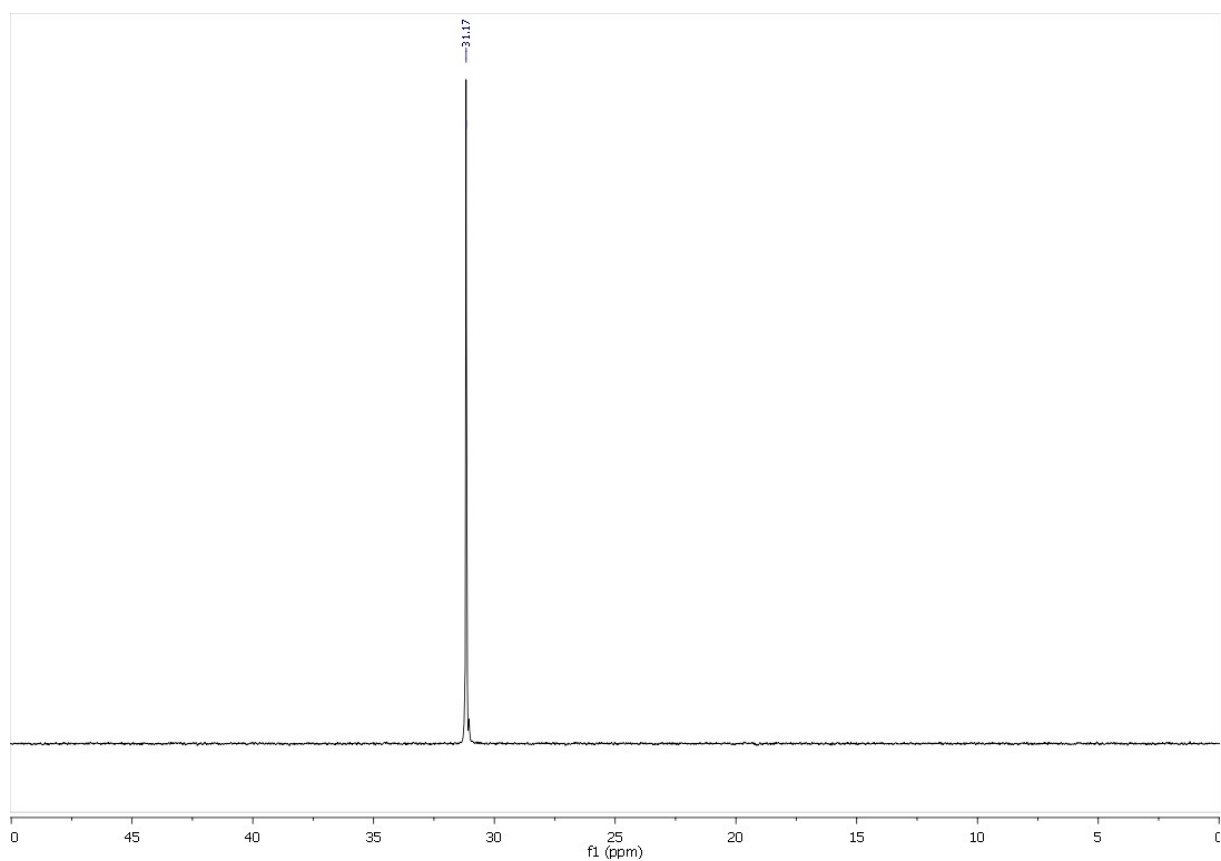


Fig. S4. $^{31}\text{P}\{^1\text{H}\}$ NMR spectrum of **P3HTPMe₃,DS** in CD_3OD .

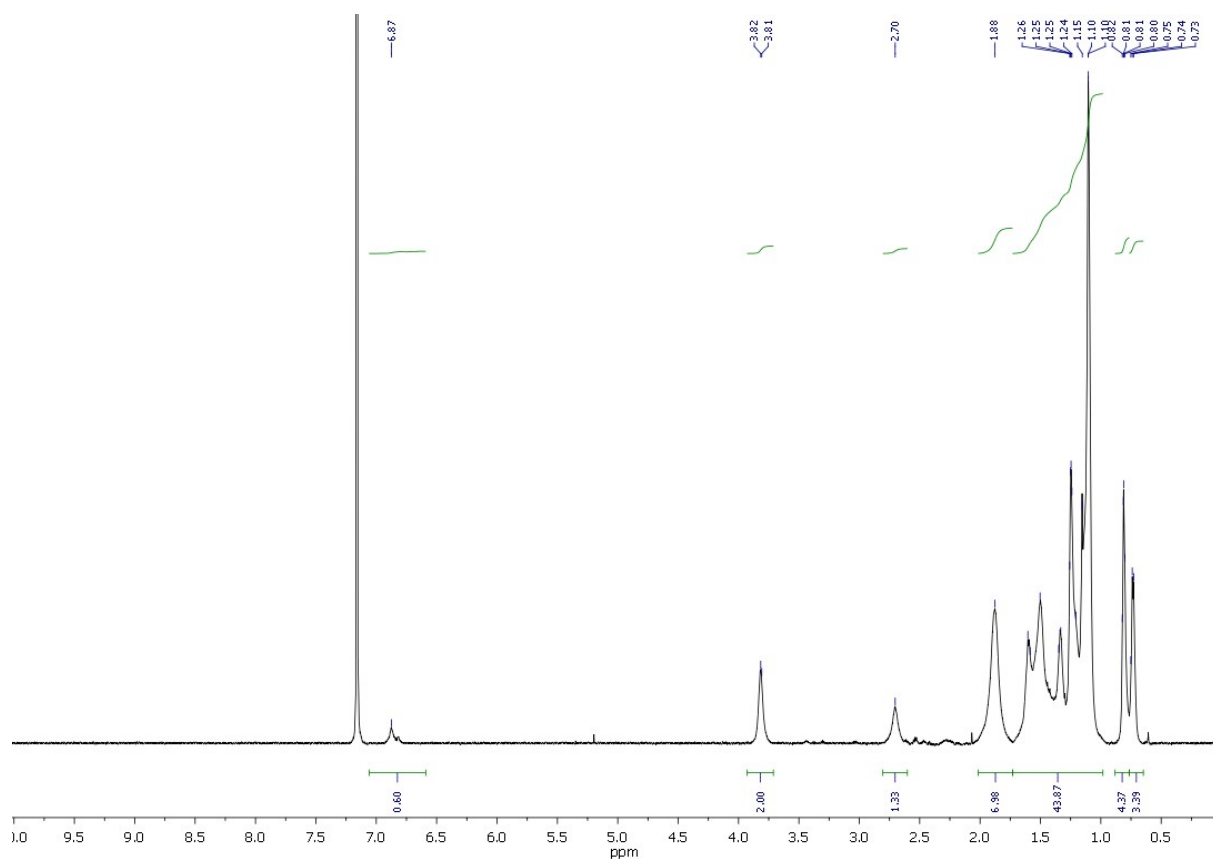


Fig. S5. ^1H NMR spectrum of **P3HT-*b*-P3HTPMe₃,DS** in CDCl_3 .

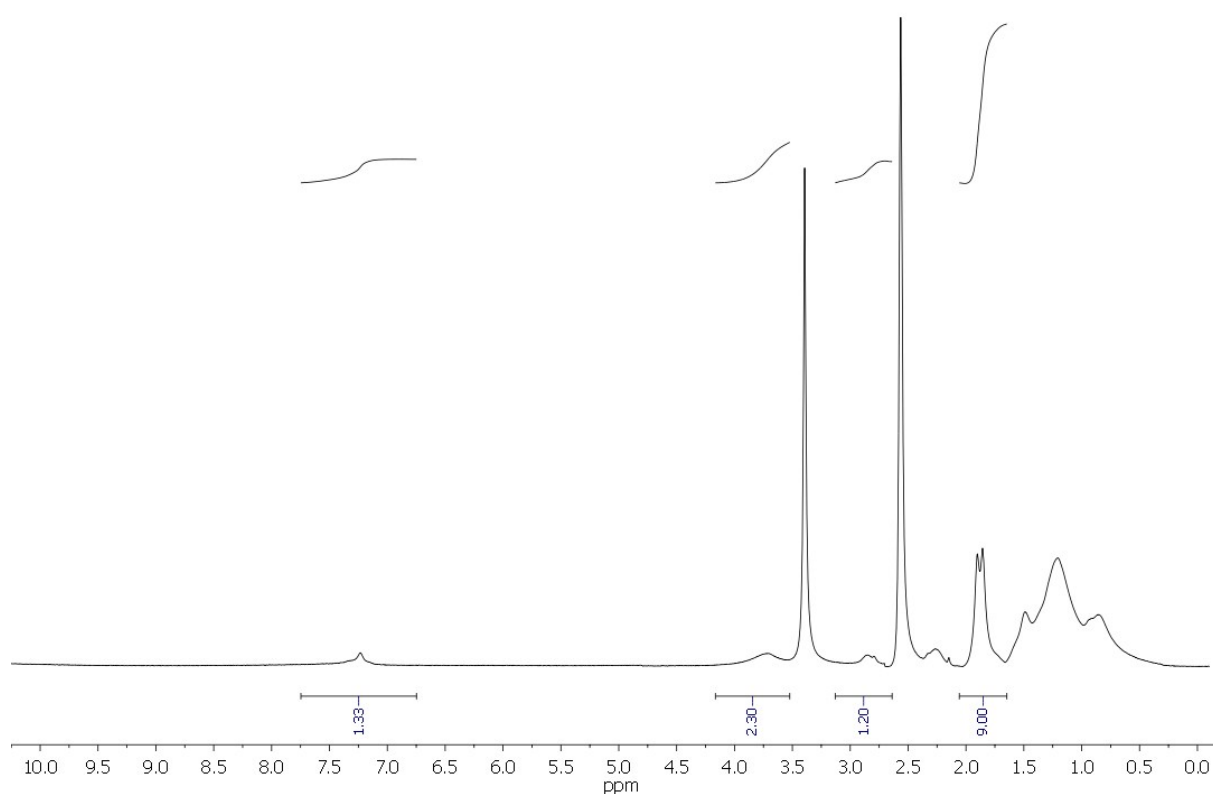


Fig. S6. ^1H NMR spectrum of **P3HT-*b*-P3HTPMe₃,DS** in $\text{DMSO-}d_6$.

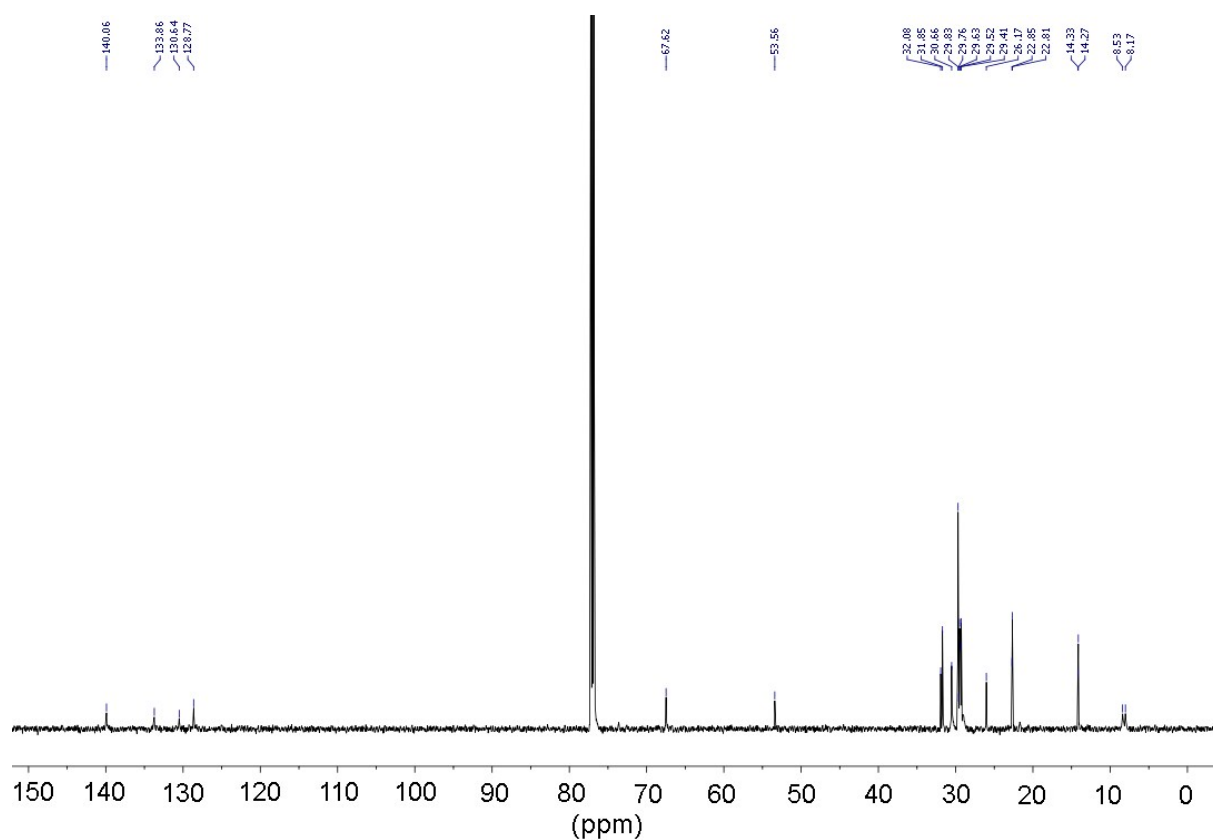


Fig. S7. $^{13}\text{C}\{^1\text{H}\}$ NMR spectrum of **P3HT-*b*-P3HTPMe₃,DS** in CDCl_3 .

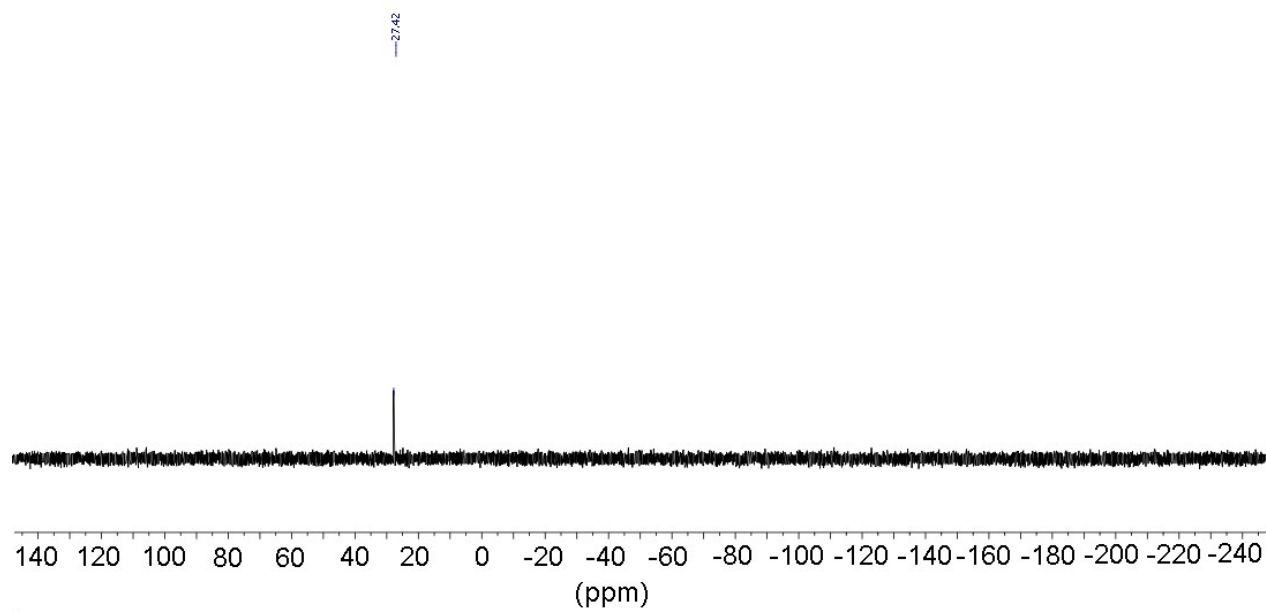


Fig. S8. $^{31}\text{P}\{^1\text{H}\}$ NMR spectrum of **P3HT-*b*-P3HTPMe₃,DS** in CDCl_3 .

SANS Data Analysis

In all cases, the solvent background was fixed for *d*₄-MeOD with a scattering length density (SLD) of $5.8 \times 10^{-6} \text{ \AA}^{-2}$. Instrumental *q*-smearing was applied between 0.001 and 0.02 \AA^{-1} to provide better fits at the high *q* end of the SANS data. Where possible the fits were checked to have absolute SANS intensities consistent with the known sample concentrations (1 vol% dry material). (NB. This check was not possible for the lamellar sheet model as the fitting only resulted in thicknesses and not lengths of sheets.) Full details of the models used in this study are described below.

The Rigid Cylinder Model

The SANS scattering profile for **P3HTPMe₃** was modelled using the Cylinder model in the SasView programme using a non-linear least squares method. The scattered SANS intensity is given by $I(q) = NV^2P(q)S(q) + bkg$, where *N* is the number of particles per unit volume, *V* is the volume of the aggregate, *P*(*q*) is the form or shape factor, *S*(*q*) is the structure factor and *bkg* is the background level.

The form or shape factor, *P*(*q*, α), for the Cylinder model is given by:¹

$$P(q, \alpha) = \frac{scale}{V} \int_0^{\pi/2} f^2(q) \sin \alpha d\alpha + bkg \quad (1)$$

where

$$f(q) = 2V(\Delta\rho) \frac{J_1(qr \sin \alpha) \sin\left(\frac{qL \cos \alpha}{2}\right)}{qr \sin \alpha \frac{qL \cos \alpha}{2}} \quad (2)$$

¹ (a) A. Guinier and G. Fournet, in *Small-Angle Scattering of X-Rays*, John Wiley and Sons: New York, 1955; (b) A. A. Golosova, J. Adelsberger, A. Sepe, M. A. Niedermeier, P. Lindner, S. S. Funari, R. Jordan and C. M. Papadakis, *J. Mater. Chem. C*, 2012, **116**, 15765.

where α is the angle between the axis of the cylinder and the q -vector, V is the total volume of the cylinder, L is the length, r is the radius, $\Delta\rho$ (contrast) is the difference in scattering length density between the scatterer (cylinder) and the solvent, and bk_g is the background level. J_1 is the first order Bessel function. The form factor is normalised by the particle volume so that the scale factor of the fit is the total particle volume fraction $\phi = NV_s$ when $I(q)$ has been correctly reduced to absolute units. The interparticle structure factor, $S(q)$, which accounts for the interference of scattering from different particles in concentrated suspensions, is assumed to be one.

The Flexible Cylinder Model

The SANS scattering profile for **P3HTPMe₃** was also modelled using the Flexible Cylinder model. This model is based on the form factor for a rigid cylinder. A chain of contour length (total length), L , can be described as a chain of some number of locally stiff segments of persistence length, I_p . I_p is the length along the cylinder over which the flexible cylinder can be considered a rigid rod. The Kuhn length, b , in this model is also used to describe the stiffness of a chain, and is simply $b = 2 \times I_p$.

The scattering function, $I_{WC}(q,L,b,R_{CS})$, for the Flexible Cylinder model is given by:²

$$I_{WC}(q,L,b,R_{CS}) = c\Delta\rho_m^2 MS_{WC}(q,L,b)P_{CS}(q,R_{CS}) + bk_g \quad (3)$$

where L is contour length, b is the Kuhn length, R_{CS} is the circular cross sectional radius, c is the concentration, M gives the average molecular weight of the micelle, $\Delta\rho$ is the difference in scattering length density between the scatterer and the solvent, and bk_g is the background level. $P_{CS}(q,R_{CS})$ is the scattering function from the cross section of a rigid rod given by:

² (a) W.-R. Chen, P. D. Butler and L. J. Magid, *Langmuir*, 2006, **22**, 6548; (b) J. S. Pederson and P. Schurtenberger, *Macromolecules*, 1996, **29**, 7602; (c) K.-S. Jang, H. J. Lee, H.-M. Yang, E. J. An, T.-H. Kim, S.-M. Choi and J.-D. Kim, *Soft Matter*, 2008, **4**, 349.

$$P_{CS}(q, R_{CS}) = \left[\frac{2J_1(qR_{CS})}{qR_{CS}} \right]^2 \quad (4)$$

where J_1 is the first order Bessel function.

$S_{WC}(q, L, b)$ is the scattering function of a single semi-flexible chain with excluded volume effects given by:

$$\begin{aligned} S_{WC}(q, L, b) = & [1 - w(qR_g)] S_{Debye}(q, L, b) \\ & + w(q, R_g) \left[1.22(qR_g)^{-\frac{1}{0.585}} + 0.4288(qR_g)^{-\frac{2}{0.585}} - 1.651(qR_g)^{-\frac{3}{0.585}} \right] \\ & + \frac{C(n_b)}{n_b} \left\{ \frac{4}{15} + \frac{7}{15u} - \left(\frac{11}{15} + \frac{7}{15u} \right) \times \exp[-u(q, L, b)] \right\} \end{aligned} \quad (5)$$

where R_g is the radius of gyration with excluded volume effects and $w(qR_g)$ is the empirical crossover function:

$$w(x) = \frac{\left\{ 1 + \tanh \left[\frac{x - 1.532}{0.1477} \right] \right\}}{2} \quad (6)$$

$$n_b = \frac{L}{b} \quad (7)$$

For $L > 10b$, $C(n_b) = 3.06n_b^{-0.44}$ and for $L \leq 10b$, $C(n_b) = 1$.

S_{Debye} is the Debye function with $u = \langle R_g^2 \rangle q^2$

$$S_{Debye}(q, L, b) = \frac{2}{u(q, L, b)} \{ \exp[-u(q, L, b)] + u(q, L, b) - 1 \} \quad (8)$$

$$u(q, L, b) = \frac{Lb}{6} \left\{ 1 - \frac{3}{2n_b} + \frac{3}{2n_b^2} + \frac{3}{4n_b^3} [1 - \exp(-2n_b)] \right\} q^2 \quad (9)$$

$$\langle R_g^2 \rangle = \alpha(n_b)^2 \frac{bL}{6} \quad (10)$$

$$u(q,L,b) = \alpha(n_b) \frac{2bL}{6} q^2 \quad (11)$$

where $\alpha(n_b)$ is the expression factor which follows the following empirical expression:

$$\alpha(x) = \sqrt{\left[1 + \left(\frac{x}{3.12}\right)^2 + \left(\frac{x}{8.67}\right)^3\right]^{0.176/3}} \quad (12)$$

The Lamellar Sheet Model

The SANS scattering profile for **P3HTPMe₃,DS** was modelled using the Lamellar model in the SasView programme using a non-linear least squares method.

The scattered SANS intensity is given by $I(q) = [2\pi VP(q)S(q)]/(dq^2) + bkg$, where V is the scattering volume, d is the lamellar spacing and bkg is the background level. The interparticle structure factor, $S(q)$, which accounts for the interference of scattering from different particles in concentrated suspensions, is assumed to be one. The form factor, $P(q)$, for neutron scattering from lamellar sheets is given by:³

$$P(q) = \frac{2\Delta\rho^2}{q^2} (1 - \cos(q\delta)) e^{-q^2\sigma^2/2}$$

(13)

where $\Delta\rho^2$ is the difference in scattering length density between the scatterer (cylinder) and the solvent (*i.e.* the contrast), δ is the bilayer thickness and σ is arbitrarily fixed at $\delta/4$.

The Core Shell Cylinder Model

The SANS scattering profiles for **P3HT-*b*-P3HTPMe₃** and **P3HT-*b*-P3HTPMe₃,DS** were modelled using a Core Shell Cylinder model in the SasView programme using a non-linear least squares method.

The scattered SANS intensity is given by $I(q) = NV_s^2P(q)S(q) + bkg$, where N is the number of particles per unit volume, V_s is the total volume of the core plus shell, P is the form or shape factor, S is the structure factor and bkg is the background level.

The form or shape factor, $P(q, \alpha)$, for the Core Shell Cylinder model is given by:⁴

$$\phi V_s P(q, \alpha) = \frac{scale}{V_s} \int_0^{\pi/2} f^2(q) d\alpha$$

(14)

³ (a) J. Berghausen, J. Zipfel, P. Lindner and W. Richtering, *J. Phys. Chem. B*, 2001, **105**, 11081; (b) F. Nallet, R. Laversanne, D. Roux, *J. Phys. II France*, 1993, **3**, 487.

where:

$$f(q) = \frac{2(\rho_c - \rho_s)V_c \sin \left[qL \cos \left(\frac{\alpha}{2} \right) \right]}{\left[qL \cos \left(\frac{\alpha}{2} \right) \right] \frac{J_1[qr \sin \alpha]}{[qr \sin \alpha]}} + \frac{2(\rho_s - \rho_{solv})V_s \sin \left[q(L+t) \cos \left(\frac{\alpha}{2} \right) \right]}{\left[q(L+t) \cos \left(\frac{\alpha}{2} \right) \right] \frac{J_1[q(r+t) \sin \alpha]}{[q(r+t) \sin \alpha]}}$$

(15)

where α is the angle between the axis of the cylinder and the q -vector, V_s is the total volume of the core plus shell, V_c is the volume of the core, L is the length of the core, r is the radius of the core, t is the thickness of the shell, ρ_c , ρ_s and ρ_{solv} are the scattering length densities of the core, shell and solvent, respectively, and bkg is the background level.⁴ J_1 is the first order Bessel function. This model provides the form factor for a circular cylinder with a core-shell scattering length density profile. The form factor is normalised by the particle volume so that the scale factor of the fit is the total particle volume fraction $\varphi = NV_s$ when $I(q)$ has been correctly reduced to absolute units. The interparticle structure factor, $S(q)$, which accounts for the interference of scattering from different particles in concentrated suspensions, is assumed to be one. The concentration of the samples is notionally low (10 mg mL^{-1}), though the solvent included in the aggregates makes the effective volume fraction much higher, and their relatively large size pushes any $S(q)$ to very low q . Attractive interactions would make $S(q)$ pull up the scattering at smallest q , in the same manner as for any larger aggregates that may form. The fitting procedure included polydispersity in the length and the radius of the rods and instrumental q smearing was applied to provide better fits at the high q end of the SANS data.

⁴ I. Livsey, *J. Chem. Soc. Faraday Trans. 2*, 1987, **83**, 1445.

Aggregation numbers

To calculate the number of **P3HTPMe₃** chains in the average cylinder particle we used the following:

$$N_{agg} = \frac{V_{dry-cylinder}}{V_{molar}} \times N_A \quad (16)$$

where N_{agg} is the aggregation number, $V_{dry-cylinder}$ is the volume of the dry cylinder, V_{molar} is the molar volume and N_A is Avogadro's number.

To calculate the number of **P3HT-*b*-P3HTPMe₃** chains in an average core-shell cylinder particle we used the following:

$$N_{agg} = \frac{V_{dry-core} + V_{dry-shell}}{V_{molar}} \times N_A \quad (17)$$

where $V_{dry-core}$ is the volume of the dry core and $V_{dry-shell}$ is the volume of the dry shell.

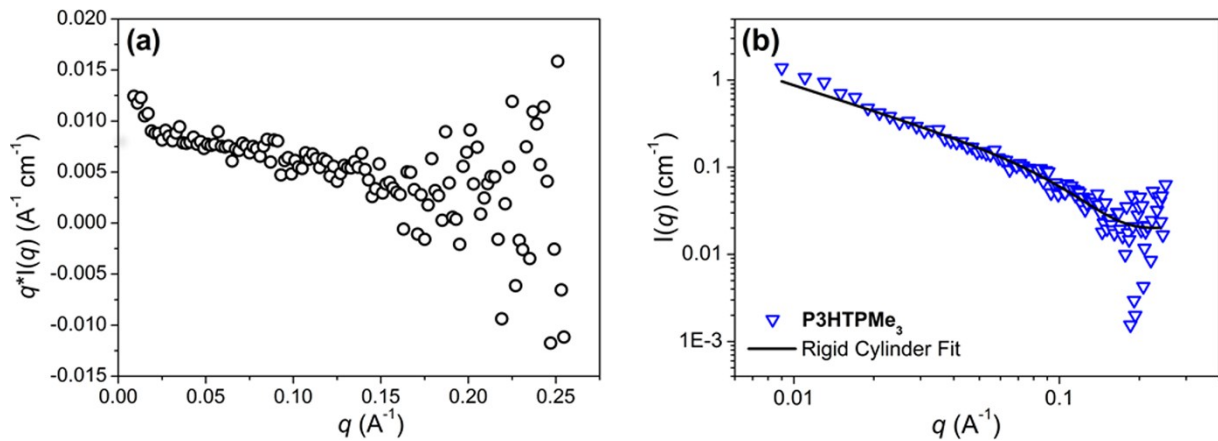


Fig. S9. (a) Holtzer or “bending rod” plot for **P3HTPMe₃** in d_4 -MeOD. (b) SANS data for **P3HTPMe₃** in d_4 -MeOD fitted with the Rigid Cylinder Model (black line) showing a poor fit at low q ($q < 0.02 \text{ \AA}^{-1}$).

Table S1. Structural parameters obtained from SANS data for **P3HTPMe₃** in *d*₄-MeOD: SLD_{sol} is the scattering length density of the solvent and α is the scattering power of the defined q region. L , r and L_{Kuhn} are the length, radius and Kuhn length, respectively, obtained from the best fits to the data using the Cylinder and the Flexible Rod Model in SasView. $X_{sol-rod}$ is the calculated solvent fraction in the cylinder aggregate.

Sample	SLD _{sol} (Å ⁻²)	$q^{-\alpha}$ ($q < 0.08$)	Model	L (Å)	r (Å)	L_{Kuhn} (Å)	$X_{sol-rod}$
P3HTPMe₃	5.8×10^{-6}	-1.22 ± 0.02	Cylinder	2865	12.9	-	0.79
			Flexible Cylinder	900.5	12.9	225.6	0.85

Table S2. Structural parameters obtained from SANS data for **P3HTPMe₃,DS** in *d*₄-MeOD: SLD_{sol} is the scattering length density of the solvent and α is the scattering power of the defined q region. T_{sheet} is the sheet thickness obtained from the best fit to the data using the Lamellar Sheet Model in SasView. $X_{sol-sheet}$ is the calculated solvent fraction in the sheet aggregate.

Sample	SLD _{sol} (Å ⁻²)	$q^{-\alpha}$ ($q < 0.02$)	$q^{-\alpha}$ ($0.02 < q < 0.07$)	Model	T_{sheet} (Å)	$X_{sol-sheet}$
P3HTPMe₃,DS	5.8×10^{-6}	-1.86 ± 0.04	-2.50 ± 0.04	Lamellar Sheet	47.2	~0.50

Table S3. Structural parameters obtained from SANS data for **P3HT-*b*-P3HTPMe₃** and **P3HT-*b*-P3HTPMe₃,DS** in *d*₄-MeOD: SLD_{sol} is the scattering length density of the solvent, α is the scattering power of the defined q region. L_{core} , r_{core} and T_{shell} are the core length, core radius and shell thickness, respectively, obtained from the best fits to the data using the Core-Shell-Cylinder Model in SasView. $X_{\text{sol-core}}$ and $X_{\text{sol-shell}}$ are the calculated solvent fractions in the core and shell, respectively.

Sample	SLD _{sol} (Å ⁻²)	$q^{-\alpha}$ ($q < 0.02$)	$q^{-\alpha}$ ($0.02 < q < 0.07$)	$q^{-\alpha}$ ($q > 0.07$)	L_{core} (Å)	r_{core} (Å)	T_{shell} (Å)	$X_{\text{sol-core}}$	$X_{\text{sol-shell}}$
P3HT-<i>b</i>-P3HTPMe₃	5.8×10^{-6}	-1.81 ± 0.10	-4.39 ± 0.05	-1.90 ± 0.13	572.8	53.1	77.4	0.15	0.86
P3HT-<i>b</i>-P3HTPMe₃,DS	5.8×10^{-6}	-1.82 ± 0.07	-4.93 ± 0.04	-1.64 ± 0.14	544.4	54.3	74.0	0.19	0.85